Allyl Isothiocyanate and Its N-Acetylcysteine Conjugate Suppress Metastasis *via* Inhibition of Invasion, Migration, and Matrix Metalloproteinase-2/-9 Activities in SK-Hep1 Human Hepatoma Cells

EUN-SUN HWANG AND HYONG JOO LEE[1]

School of Agricultural Biotechnology and Center for Agricultural Biomaterials, College of Agriculture and Life Sciences, Seoul National University, Shillim-dong, Gwanak-gu 151-742, Republic of Korea

Cruciferous vegetables contain a series of relatively unique secondary metabolites of amino acids, called glucosinolates. Sinigrin, the predominant aliphatic glucosinolate in cruciferous vegetables, is hydrolyzed to yield allyl isothiocyanate (AITC), which, after absorption and metabolism in humans, is excreted in the urine as an N-acetylcysteine (NAC) conjugate. We have determined the inhibitory effects of AITC and its NAC conjugate on cell proliferation, the expression of matrix metalloproteinases (MMPs), adhesion, invasion, and migration in SK-Hep1 human hepatoma cells. Our results demonstrate that AITC and NAC-AITC suppress SK-Hep1 cell proliferation in a dose-dependent manner; by 25% and 30% for 10 μ*M* AITC and 10 μ*M* NAC-AITC, respectively. We examined the influence of AITC and NAC-AITC on the gene expression of MMPs and tissue inhibitors of metalloproteinase (TIMPs). Gelatin zymography also revealed a significant downregulation of MMP-2/-9 expression in SK-Hep1 cells treated with 0.1–5 μ*M* AITC and NAC-AITC compared with controls. Reverse transcriptase polymerase chain reaction revealed dose-dependent decreases in MMP-2/-9 messenger RNA levels in both AITC-treated and NAC-AITC–treated cells. TIMP-1/-2 activities were unaffected by treatment with AITC or NAC-AITC in our experiments. NAC-AITC inhibited cancer cell adhesion and invasion much more potently than its parent compound. NAC-AITC at 5 μ*M* caused excellent inhibition of cell migration for 48 hrs. These results demonstrate the potential of AITC and NAC-AITC as chemopreventive agents.
Exp Biol Med 231:421–430, 2006

Key words: allyl isothiocyanate; sinigrin; *N*-acetylcysteine; SK-Hep1 cells; adhesion; invasion; migration; metastasis; matrix metalloproteinase; tissue inhibitors of metalloproteinase

Introduction

Glucosinolates are naturally occurring thioglucosides that are present in cruciferous vegetables, such as Brussels sprouts, broccoli, cabbage, cauliflower, turnip, radish, and watercress (1). Although glucosinolates are not thought to be directly bioactive, their enzymatic hydrolysis products, isothiocyanates (ITCs), seem to exhibit anticarcinogenic activity. The predominant glucosinolate in some cruciferous vegetables is sinigrin, which is hydrolyzed to allyl ITC (AITC; Ref. 2). Once absorbed, the primary metabolic route for AITC is conjugation with glutathione followed by conversion *via* the mercapturic acid pathway to an N-acetylcysteine (NAC) conjugate (NAC-AITC) that is excreted into the urine (3, 4). Thus, the presence of NAC-AITC in the urine indicates uptake and metabolism of AITC in the body.

AITC has been shown to induce strong glutathione-*S*-transferase and quinine reductase activities (5, 6). Naturally occurring AITC has also been implicated in the inhibition of B16F-10 melanoma cell–induced metastasis and tumor colony formation by 93% after 21 days of tumor induction in C57BL/6 mice (7); there was also a corresponding increase in the lifespan of AITC-treated animals. These results suggest that naturally occurring AITC is a class of promising chemopreventive agents that could play important roles in modulating the activation and detoxification of

This work was supported by Korea Research Foundation Grants (KRF-2004-005-F00055 and KRF-2005-206-F00008) funded by the Korean Ministry for Education and Human Resources Development.

[1] To whom correspondence should be addressed at Department of Food Science and Technology, School of Agricultural Biotechnology and Center for Agricultural Biomaterials, College of Agriculture and Life Sciences, Seoul National University, San 56-1, Shillim-dong, Gwanak-gu, Seoul 151-742, Republic of Korea. E-mail: leehyjo@snu.ac.kr

Received November 21, 2005.
Accepted January 4, 2006.

1535-3702/06/2314-0421$15.00

carcinogenesis. Hwang and Jeffery (4) confirmed that AITC is conjugated with glutathione and excreted as NAC-AITC in rat and human urine after the consumption of Brussels sprouts. Several researchers have suggested that the NAC conjugate of an ITC is as effective, or more effective, than free ITC (8, 9). The free form and the NAC-conjugated form of sulforaphane (NAC-sulforaphane) and the NAC conjugate of phenethyl ITC (NAC-PEITC) have previously been shown to inhibit cancer cell growth and induce Phase II detoxification enzyme in culture (10–12). Furthermore, NAC-sulforaphane and NAC-PEITC are reported also to be effective when administered *in vivo* (13). Therefore, NAC-AITC may be an effective chemopreventive agent.

Metastasis is one of the major causes of mortality in cancer patients, and occurs as a complex multistep process involving cancer cell adhesion, invasion, and migration (14). The degradation of environmental barriers, such as the extracellular matrix (ECM) and basement membrane is an initial step of this process, and several proteolytic enzymes participate in degrading these barriers (15), with matrix metalloproteinases (MMPs) playing a major role. MMPs are a family of zinc-binding endopeptidases that collectively degrade most of the components of ECM, and they have been implicated in cancer invasion and metastasis (16). In particular, MMP-2 and -9 degrade components of the basement membrane and are strongly implicated in the invasion and metastasis of malignant tumors (16, 17). Therefore, inhibition of MMP activity is important in cancer cell metastasis, mostly affecting cancer development after carcinogenesis. The proteolytic activities of MMPs are controlled by their endogenous inhibitors, the tissue inhibitors of metalloproteinases (TIMPs; Ref. 18). It has been proposed that the activity of MMPs is related to the ratios of the concentrations of MMP-2 to TIMP-2 and of MMP-9 to TIMP-1 (19).

Under physiologic conditions, the regulation of the MMP family may be under the control of gene expression, proenzyme activation, and interaction with specific inhibitors, such as tissue-specific inhibitors (e.g., TIMPs; Refs. 20, 21). Four TIMP members have been identified (designated as TIMP-1, -2, -3, and -4), and they interact with MMPs stoichiometrically (on a 1:1 molar basis; Refs. 21, 22). Thus, TIMPs provide a regulated mechanism for controlling MMP activation and function. MMPs and TIMPs have been studied in prostate tumors grown in animals (23, 24), in malignant prostate cells (25, 26), and in cell cultures of human prostate tissue (27, 28). Increased MMP-2 and -9 and reduced TIMP-1 concentrations were found in conditioned media of epithelial cultures from the neoplastic prostate (29).

The aim of the present study was to use gelatin zymography to elucidate the potential of AITC and NAC-AITC in inhibiting the activities of MMP-2 and -9. We examined the expression of the messenger RNAs (mRNAs) of MMP-2 and -9 relative to their corresponding TIMPs in SK-Hep1 cells. We also investigated the influence of AITC and NAC-AITC on the viability, adhesion, invasion, and migration of SK-Hep1 cells.

Materials and Methods

Chemicals. Dulbecco's modified Eagle's medium (DMEM), 3-(4,5-dimethylthiazol-2-yl)-2,5-diphenyltetrazolium bromide (MTT), and RNase A were obtained from Sigma Chemical (St. Louis, MO). Trypsin-EDTA and penicillin/streptomycin were obtained from Gibco Life Technologies (Paisley, UK), and fetal bovine serum (FBS) was obtained from Gemini Bio-Products (Calabasas, CA). All solvents were of analytical high-performance liquid chromatography grade (Fisher Scientific, Los Angeles, CA), and cell culture supplies were purchased from Costar (Corning, Cypress, CA) and Sigma Chemical. AITC (99%) was purchased from ACROS Organics (Geel, Belgium).

Cell Culture. SK-Hep1 human hepatoma cells were obtained from Korean Cell Line Bank (Seoul, Korea). SK-Hep1 cells were cultured in DMEM supplemented with 10% FBS and penicillin/streptomycin in a 37°C humidified incubator containing 5% CO_2 and 95% air.

Synthesis of NAC-AITC. NAC-AITC was synthesized using a published method (4). The synthesized product was analyzed with tandem mass spectrometry coupled with an electrospray ionization source (Quattro Micro, Manchester, UK) that was used with the following settings: capillary voltage of 4.2 kV, source temperature of 1207°C, desolvation temperature of 240°C, desolvation nitrogen gas flow rate of 650 l/hr, and an argon gas pressure of 2.5 mbar (used as the collision gas).

Cell Proliferation Assay. The MTT assay was used to quantify cell viability. Briefly, cells (5×10^3 cells/well) were cultured in 96-well plates at 37°C. After 24 hrs of incubation, all medium was removed, and the well was filled with fresh FBS-free medium containing various amounts of AITC or NAC-AITC. The cells were then incubated for 24–72 hrs, all medium was removed, and cell viability was evaluated as follows. MTT was dissolved in phosphate-buffered saline (PBS) at 5 mg/ml and filtered to sterilize the solution and remove the small amounts of insoluble residue. A mixture comprising 10 µl of the MTT stock solution and 90 µl of medium was added to each well of the 96-well plate culture. After the plates were incubated for 4 hrs at 37°C, DMSO was added to the wells and mixed by pipetting to dissolve the dark blue formazan product. The optical density at 570 nm of each well was determined using a microplate reader (Molecular Devices, Sunnyvale, CA).

Cell Adhesion Assay. Twenty-four-well tissue culture plates were coated with Matrigel (Sigma Chemical) at 25 µg/well and left to air-dry for 40 mins. Cells (5×10^4) suspended in DMEM containing 0.5% bovine serum albumin with AITC or NAC-AITC were dispensed into each well of a 24-well culture plate, incubated in 5% CO_2 at 37°C for 1 hr, and gently washed three times with PBS to

Table 1. Sequences of Primers Used in This Study

Target gene	Primer	Sequence (5′ → 3′)	Product size (bp)
MMP-2	Sense	GGC CCT GTC ACT CCT GAG AT	474
	Antisense	GGC ATC CAG GTT ATC GGG GA	
MMP-9	Sense	CGG AGC ACG GAG ACG GGT AT	573
	Antisense	TGA AGG GGA AGA CGC ACA GC	
TIMP-1	Sense	GAT CCA GCG CCC AGA GAG ACA CC	677
	Antisense	TTC CAC TCC GGG CAG CAT T	
TIMP-2	Sense	GGC GTT TTG CAA TGC AGA TGT AG	500
	Antisense	CAC AGG AGC CGT CAC TTC TCT TG	
GAPDH	Sense	TGA AGG TCG GAG TCA ACG GAT TTG GT	983
	Antisense	CAT GTG GGC CAT GAG GTC CAC CAC	

remove the unattached cells. Cells attached to the bottom of plate were stained with hematoxylin-eosin reagent and counted under an Olympus Ix70 microscope (Olympus, Okaya, Japan). Each experiment was independently performed at least four times.

Cell Invasion Assay. A Transwell system with a polycarbonate filter membrane 6.5 mm in diameter and an 8-μm pore size (Corning, Corning, NY) was used to assess the rate of cell invasion. Matrigel (12.5 μg in 50 μl PBS) was added to the filter to form a thin gel layer, dried in a laminar hood overnight, and reconstituted with 100 μl of PBS at 37°C for 2 hrs. The cells that were 90% confluent were harvested by cell dissociation solution. Cells (1×10^5) suspended in 100 μl of serum-free medium—with or without treatment compounds at different concentrations—were added to the upper chamber of the Transwell insert, and the lower chamber was filled with 500 μl of the same medium. After a 24 hrs of incubation at 37°C, the cells on the upper surface of the filter were completely wiped off with a cotton swab. The cells that penetrated to the lower surface of the filter were stained with hematoxylin-eosin and counted under a microscope (Olympus Ix70) in 13 randomized fields at a ×400 magnification. The assay was performed in at least four independent experiments.

Wound Migration Assay. Cell migration was examined using a wound migration assay. Cells were cultured in six-well plates to 100% confluency, and pretreated with mitomycin C (25 μg/ml) for 30 mins before a plastic pipet tip was used to produce a clean 1-mm-wide wound area across the center of the well. After being rinsed with PBS, the cells were allowed to migrate in the medium. A computer-based microscopy imaging system (Olympus) was used to assess the wound at 0 hr at ×200 magnification. The migration was assessed at specific time points by quantifying the number of cells observed across the wound relative to the same position at 0 hr. At least five wound areas were investigated on each plate to quantify the migration. The migration distances between the leading edge of the migrating cells and the edge of the wound were compared. The migration rate was quantified as the following equation: migration rate = (migration distance of AITC-treated or NAC-AITC–treated cells / migration distance of untreated control cells) × 100%. Experiments were independently performed at least four times.

Gelatin Zymography. The gelatinase activity was determined by gelatin zymography as described previously (30). Briefly, SK-Hep1 cells were incubated with 0–5 μ*M* AITC or NAC-AITC in serum-free DMEM for 48 hrs. Conditioned media were collected, and the protein level was determined. Protein-standardized conditioned media were resolved using 10% sodium dodecyl sulfate (SDS) polyacrylamide gel electrophoresis containing 1 mg/ml gelatin. Electrophoresis was performed at a constant voltage of 105 V. After electrophoresis, the gel was washed two times with 2.5% Triton X-100 for 30 mins to remove SDS, and the gel was subsequently incubated in buffer containing 50 m*M* Tris-HCl (pH 7.6), 200 m*M* NaCl, and 5 m*M* $CaCl_2$ for 18 hrs at 37°C. The gel was stained with 0.5% Coomassie blue for 1 hr and destained in water containing 10% glacial acetic acid and 30% methanol. Proteolysis was detected as a white zone in a dark field, with the intensities of the bands quantified using standard software (ImageJ, v.1.34; the National Institutes of Health, Bethesda, MD).

Isolation of Total RNA. Total RNA was isolated from 10^7 cells using TRIzol reagent (Life Technologies, Rockville, MD). The homogenized samples were incubated for 5 mins at room temperature so that the nucleoprotein complexes completely dissociated. After the addition of 0.2 volumes of chloroform, samples were shaken vigorously for 15 secs, incubated for 2–3 mins, and centrifuged at 12,000 *g* for 15 mins at 4°C. The total RNA remaining in the upper aqueous phase was precipitated by mixing with an equal volume of isopropanol. The mixtures were then incubated for 10 mins at 4°C and centrifuged at 12,000 *g* for 10 mins at 4°C. The resulting total RNA pellet was washed with 70% ethanol, dried, and dissolved in RNase-free water. The concentration and purity of total RNA were calculated based on the absorbance at 260 and 280 nm.

Semiquantitative Reverse Transcriptase (RT) Polymerase Chain Reaction (PCR). The primer sets used in this study are listed in Table 1. First-strand complementary DNA (cDNA) was synthesized with 1 μg of total RNA and 1 μ*M* oligo(dT15) primer using Omniscript Reverse Transcriptase (Qiagen, Valencia, CA). Using

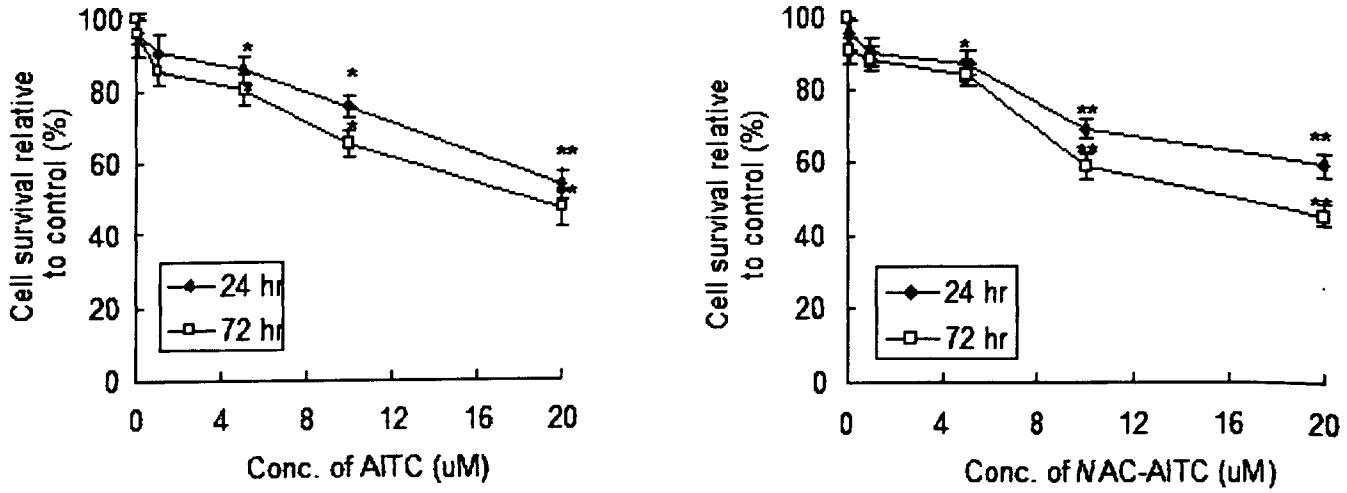

Figure 1. Effect of AITC and NAC-AITC on SK-Hep1 cell proliferation as measured by the MTT assay. The optical density was determined at 570 nm, and is expressed as cell survival relative to control. Data are mean ± SD values from four independent experiments. $^{*}P < 0.05$; $^{**}P < 0.01$, means that differ significantly from other treatments.

the Taq PCR Master Mix kit (Qiagen), subsequent PCR as performed with 0.5 μl of first-strand cDNA and 20 pmol of primers. The PCR consisted of an initial denaturation at 94°C for 3 mins; 30 three-step cycles at 94°C for 1 min, 60°C for 1 min, and 72°C for 1 min; and a final extension at 72°C for 10 mins. The amplified PCR products were loaded onto a 0.8% agarose gel. After ethidium bromide staining, the gel was illuminated on a UV transilluminator and photographed using Polaroid film (Kodak, Needham, MA). The bands intensities were measured using ImageJ.

Statistical Analysis. Each experiment was replicated three times. Means, standard deviations, mean square errors, two-way analysis of variance (ANOVA), correlations, and interactions of main effects were calculated using standard software (Sigmastat v.1.0; Jandel, San Rafael, CA). Appropriate comparisons were made using the Student-Newman-Keuls method for multiple comparisons. A probability value of $P < 0.05$ was considered statistically significant.

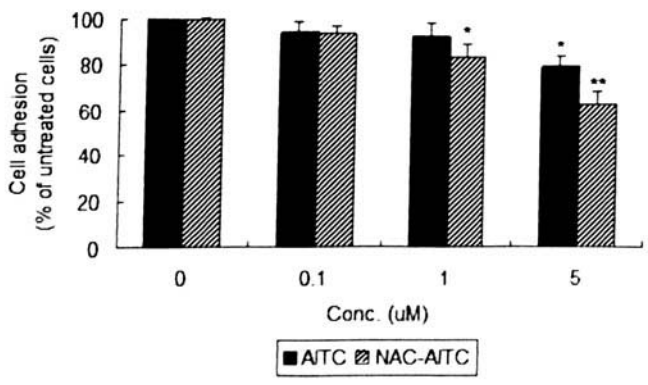

Figure 2. Effect of AITC and NAC-AITC on cell adhesion on Matrigel. SK-Hep1 cells were treated with and without AITC or NAC-AITC at different concentrations for 24 hrs in wells precoated with Matrigel. After a 60-min incubation at 37°C, the percentage of adhering cells was counted under the microscope. Data are mean ± SD values from three independent experiments. $^{*}P < 0.05$; $^{**}P < 0.01$, means that differ significantly from other treatments.

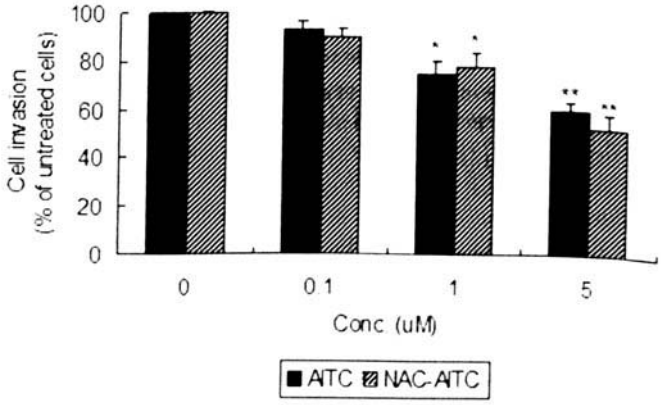

Figure 3. Effect of AITC and NAC-AITC on invasion of SK-Hep1 cells. Invasion of SK-Hep1 cells toward conditioned medium was measured using Transwell chambers with tissue culture–treated filters with 8-μm pores. Each bar represents the mean ± SD of three independent experiments. $^{*}P < 0.05$; $^{**}P < 0.01$, means that differ significantly from other treatments.

→

Figure 4. Effects of AITC and NAC-AITC on wound healing migration of SK-Hep1 cells. A wound was introduced by scraping the confluent cell layers with a pipet tip. (A) Representative photographs of invading control, AITC-treated, and NAC-AITC–treated cells. (B) Migration distances were measured at the indicated time points. Migration rate was quantified as the migration distances of AITC-treated or NAC-AITC–treated cells relative to those of control cells, expressed as a percentage. Data are mean ± SD values from four independent experiments. $^{*}P < 0.05$, means that differ significantly from the controls.

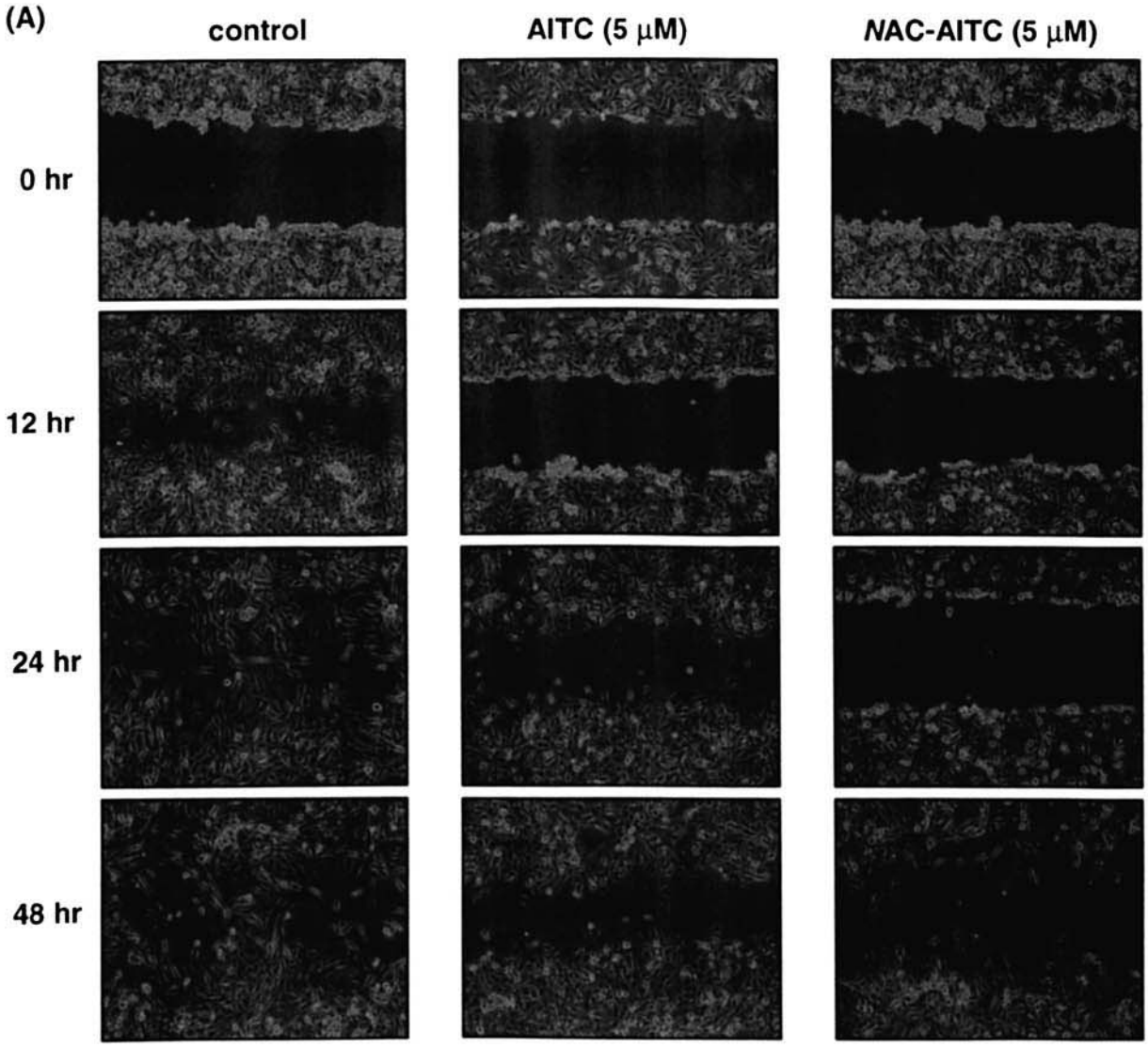
(A)
control
AITC (5 μM)
NAC-AITC (5 μM)
0 hr
12 hr
24 hr
48 hr

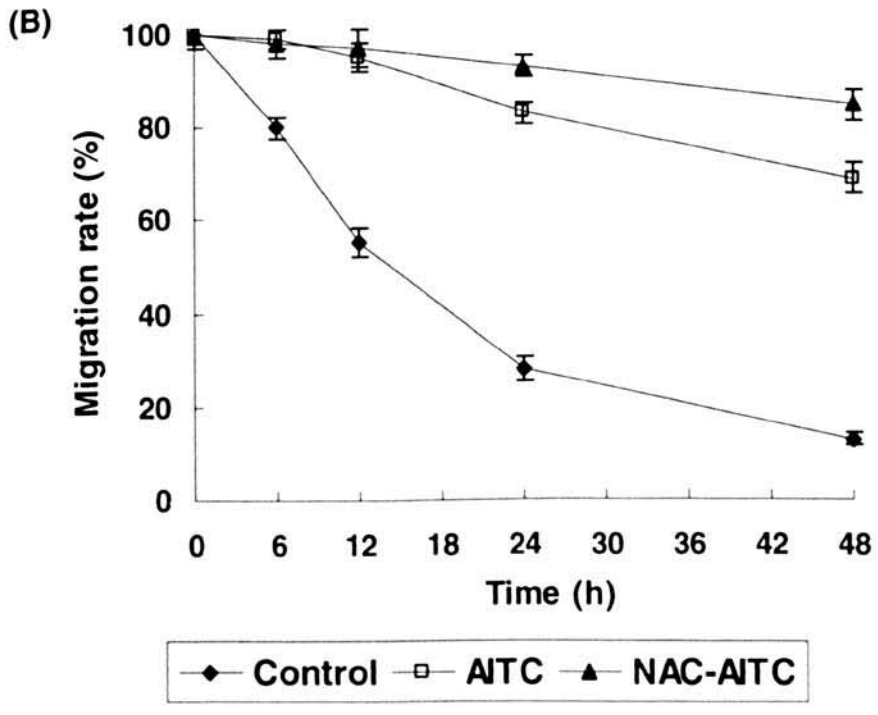
(B)
Migration rate (%)
100
80
60
40
20
0
0
6
12
18
24
30
36
42
48
Time (h)
Control
AITC
NAC-AITC

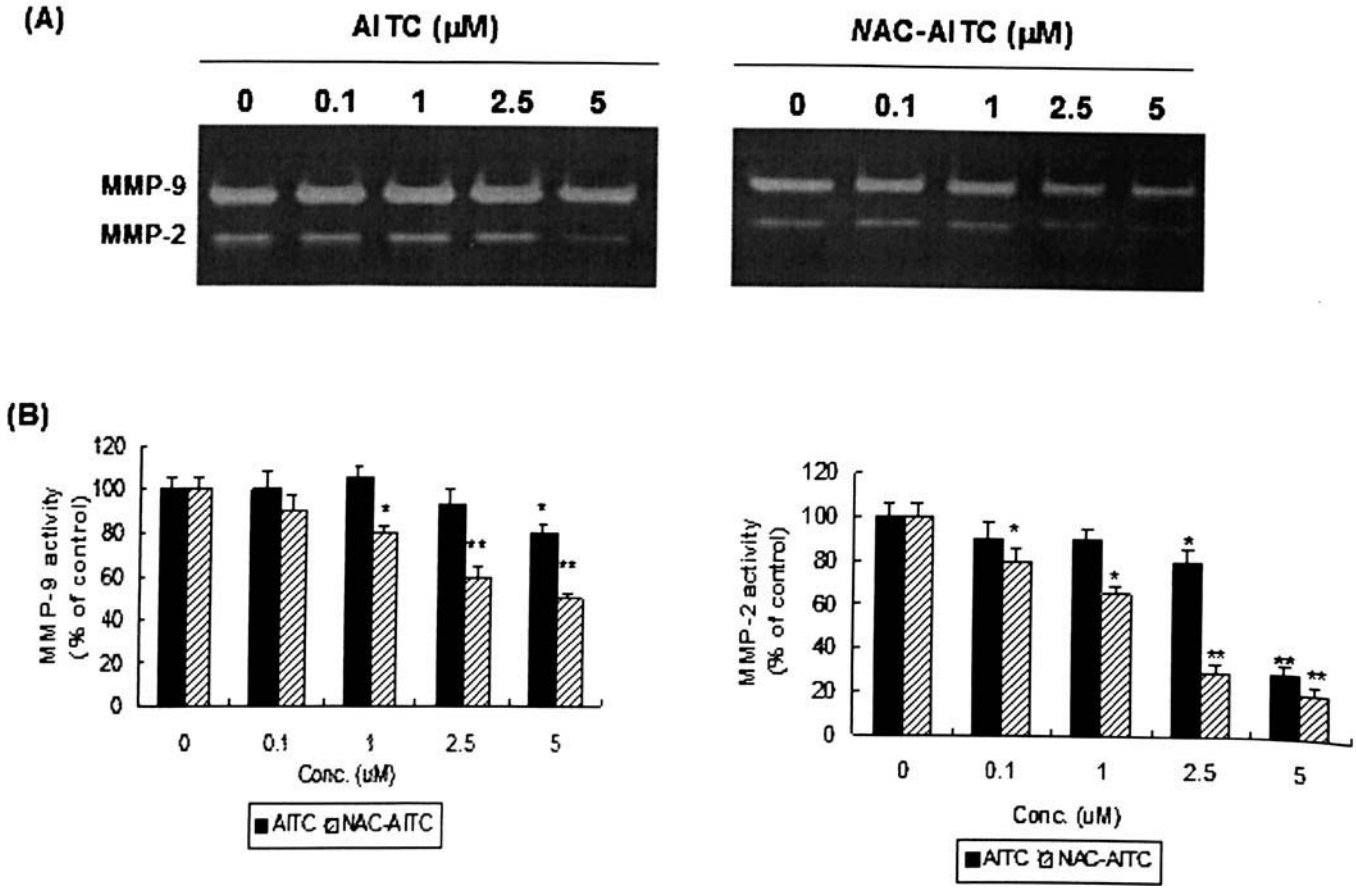

Figure 5. The expression of MMP-2/-9 was analyzed by gelatin zymography, which was performed on media conditioned by 2×10^5 SK-Hep1 cells treated with AITC or NAC-AITC for 48 hrs (A). Data shown are representative of three independent experiments that gave essentially the same results. The relative enzyme activities of MMP-2 and -9 are expressed as percentages relative to control samples (B). $^*P < 0.05$; $^{**}P < 0.01$, means that differ significantly from other treatments.

Results

The synthesized NAC-AITC exhibited a major peak in its mass spectrum at m/z = 263, corresponding to the strong molecular ion (M^+) as the major peak at 263, which is the molecular weight +1 of the NAC conjugate of AITC. A distinct M^+Na^+ peak at m/z = 285 was obtained because of the sodium ion in the matrix.

The cytotoxicity of AITC and NAC-AITC toward SK-Hep1 human hepatoma cells was evaluated using the MTT assay. Figure 1 shows the effects of 0.1–20 μ*M* AITC and 0.1–20 μ*M* NAC-AITC on the growth of SK-Hep1 cells after 24 and 72 hrs. After 24 hrs of incubation, AITC inhibited the proliferation of SK-Hep1 cells in a dose-dependent manner ($n = 4$). AITC at concentrations of 0.1–20 μ*M* significantly reduced the cell numbers compared with controls, by 4%–46%, respectively. Similarly, after 72 hrs of incubation, the cell numbers were decreased by 35% and 53% for 10 and 20 μ*M* AITC, respectively. After 24 hrs of incubation, 10 and 20 μ*M* NAC-AITC decreased cell numbers by 30% and 41%, respectively, and also dose-dependently inhibited SK-Hep1 cell proliferation.

To investigate the effect of AITC and NAC-AITC on the adhesion of SK-Hep1 cells, the number of adhesive cells was determined by an enzyme-linked immunosorbent assay reader. Incubation of SK-Hep1 cells with 0.1–5 μ*M* AITC and 0.1–5 μ*M* NAC-AITC for 60 mins significantly inhibited cell adhesion to the Matrigel-coated substrate in a concentration-dependent and linear manner (Fig. 2); the reduction was 21% and 37% with 5 μ*M* AITC and 5 μ*M* NAC-AITC, respectively.

We examined the inhibitory effect of AITC and NAC-AITC on the ability of SK-Hep1 cells to invade through reconstituted ECM (Matrigel) with or without treatment. AITC or NAC-AITC inhibited the invasion of SK-Hep1 cells in a dose-dependent manner in the range 0.1–5 μ*M*. For SK-Hep1 cells grown on Matrigel, a significant reduction ($P < 0.05$ and $P < 0.01$) in the number of invasive cells was seen when the cells were treated with AITC or NAC-AITC for 18 hrs, as compared with the control (fresh medium alone), with the levels of invasion being reduced to 60% and 53% of the control levels for 5 μ*M* AITC and 5 μ*M* NAC-AITC, respectively (Fig. 3). No significant reduction in invasiveness was observed when the cells were treated for 6 hrs with either AITC or NAC-AITC at 0.1–2.5 μ*M* (data not shown).

AITC and NAC-AITC affected wound healing migra-

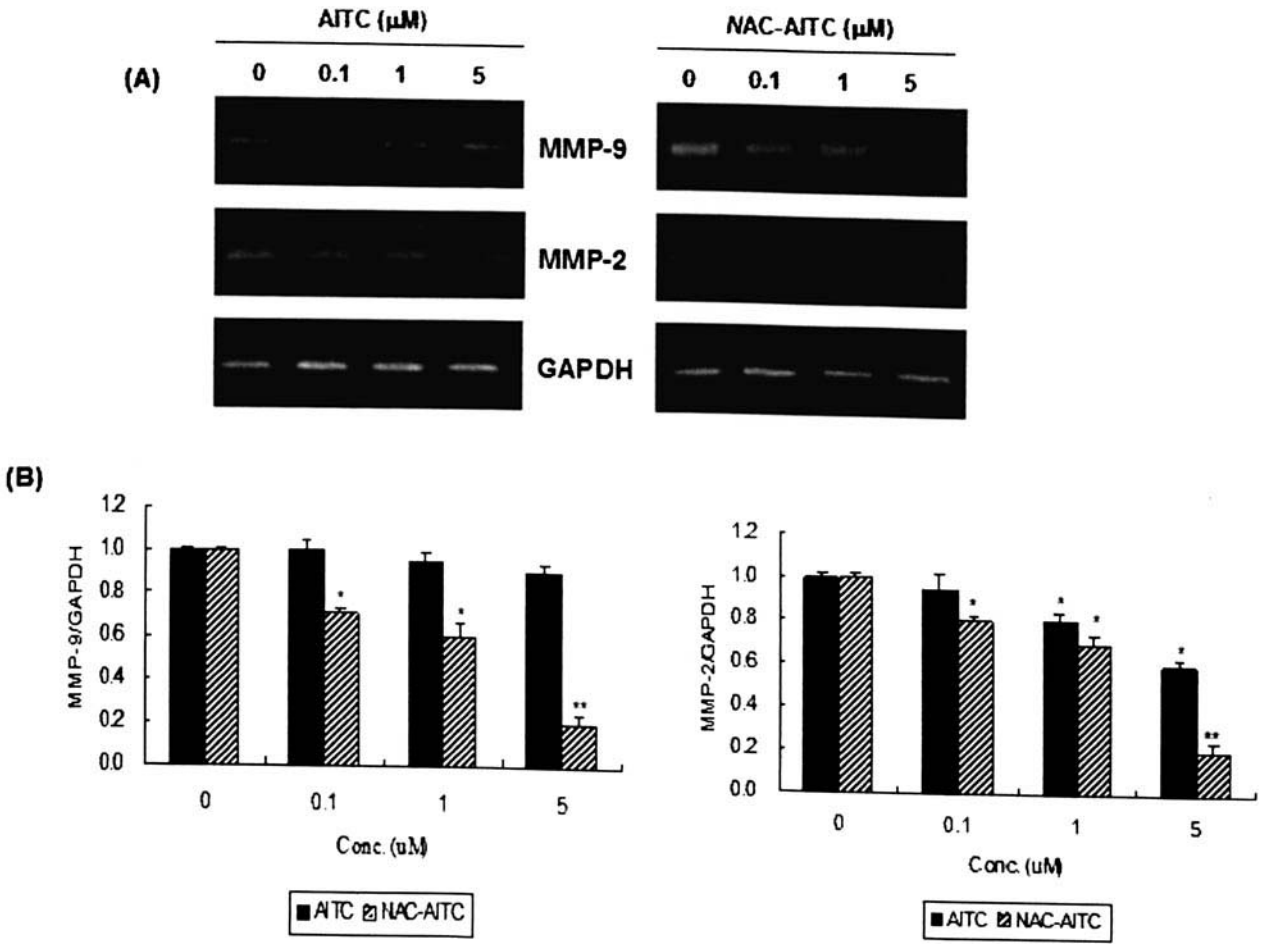

Figure 6. Expression of MMP-2/-9 mRNA in SK-Hep1 cells as determined by RT-PCR analysis after the cells were treated with AITC and NAC-AITC at different concentrations for 24 hrs. The experiment was repeated three times with similar results. (A) Photograph of an electrophoresis gel of PCR products. (B) The MMP-2/GAPDH and MMP-9/GAPDH ratios in the cells treated with AITC and NAC-AITC at different concentrations were determined by densitometry. $^{*}P < 0.05$; $^{**}P < 0.01$, means that differ significantly from other treatments.

tion of SK-Hep1 cells. The migration distances between the leading edge and the wound line were compared between AITC-treated, NAC-AITC–treated, and control cells. As shown in Figure 4, cellular migration was controlled in a time-dependent manner by 5 μM AITC, being inhibited by up to 83% and 69% at 24 and 48 hrs of incubation, respectively ($P < 0.001$). NAC-AITC at 5 μM showed similar inhibitory patterns on cell migration, but with a stronger effect than AITC at the same molar concentration; NAC-AITC inhibited the migration rates of SK-Hep1 cells inhibited by 93% and 85% at 24 and 48 hrs of incubation, respectively.

We examined the effect of AITC and NAC-AITC on the expression of MMP-2 and -9 to elucidate their possible action mechanisms of antimetastasis. Zymography revealed that the SK-Hep1 cells constitutively secreted high levels of MMP-9 and low levels of MMP-2, and that the presence of increased concentrations of AITC and NAC-AITC reduced MMP-9 and -2 activities in a dose-dependent manner (Fig. 5), with NAC-AITC showing a more potent inhibitory effect than AITC. MMP-9 activity was suppressed by 20% and 50% by treatment with 5 μM AITC and 5 μM NAC-AITC, respectively. AITC at a low concentration (<1.0 μM) did not inhibit MMP-9 expression. AITC and NAC-AITC at 5 μM suppressed MMP-2 activity by 70% and 80%, respectively, and, at concentrations of 0.1–5 μM, inhibited the activity in a dose-dependent manner.

The MMP-9 messenger RNA (mRNA) level in SK-Hep1 cells was quantified by RT-PCR with an endogenous standard (GAPDH) after cells were exposed to AITC or NAC-AITC for 24 hrs (Fig. 6). AITC at 0.1–5 μM did not suppress the MMP-9 mRNA level in SK-Hep1 cells, whereas NAC-AITC at 1 and 5 μM suppressed MMP-9 mRNA by 20% and 40%, respectively. The inhibition of MMP-2 mRNA expression was greater than that of MMP-9 mRNA, with 40% and 80% inhibition by 5 μM AITC and 5 μM NAC-AITC, respectively.

The effects of 24 hrs of exposure to AITC and NAC-AITC on TIMP-1/-2 activities in SK-Hep1 cells are shown in Figure 7. TIMP-1/-2 mRNA was expressed in control, AITC-treated, and NAC-AITC–treated cells, but there was no dose-response relationship; the TIMP-1/-2 activities were unaffected after treatment with AITC or NAC-AITC in our experiments. There were also no significant correlations

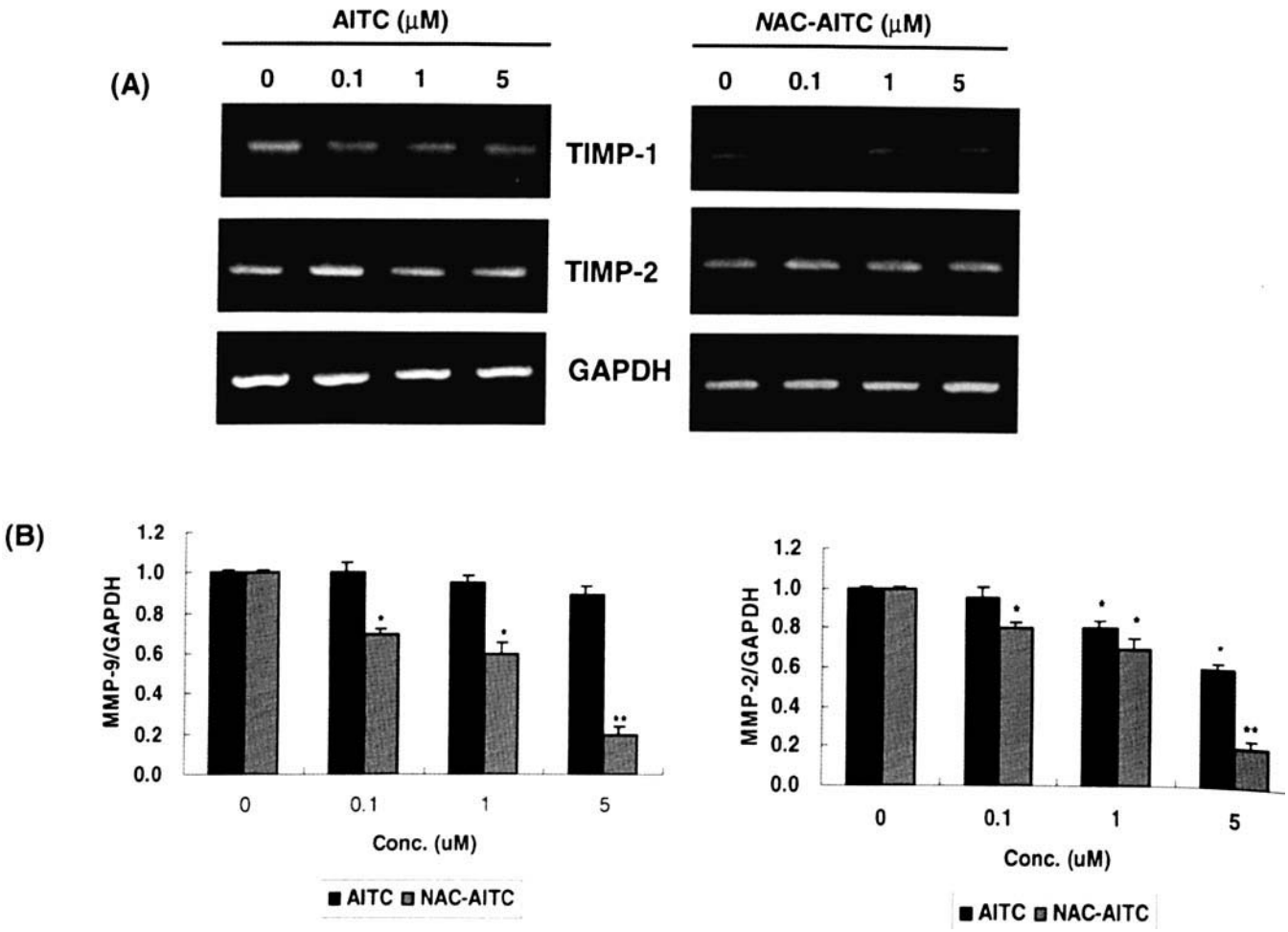

Figure 7. Expression of *TIMP*-1/-2 mRNA in SK-Hep1 cells as determined by RT-PCR analysis after the cells were treated with AITC and NAC-AITC at different concentrations for 24 hrs. The experiment was repeated three times with similar results. (A) Photograph of an electrophoresis gel of PCR products. (B) The TIMP-1/GAPDH and TIMP-2/GAPDH ratios in the cells treated with AITC and NAC-AITC at different concentrations were determined by densitometry.

between the mRNA expression and the protein expressions of MMP-2/-9 and TIMP-1/-2.

Discussion

This study provides evidence that AITC and NAC-AITC (a major metabolite of AITC from cruciferous vegetables) inhibit cancer cell proliferation, MMP expression, cell adhesion, invasion, migration, and metastasis in SK-Hep1 human hepatoma cells. Glucosinolate metabolites could be formed in the colon as a result of bacterial fermentation (19). Cooking brassica vegetables briefly at relatively low temperatures increases the yield of ITC after their consumption (31). Thus, biologically active glucosinolate-breakdown products can be derived from both raw and lightly cooked brassica vegetables. Whatever their origin, glucosinolate-breakdown products are absorbed from the gut lumen and metabolized by the intestinal epithelial cells (19).

In this study, we used SK-Hep1 human hepatoma cancer cells because liver cancer is the second most common fatal cancer in Southeast Asia and Korea. Because all experiments were conducted in a single cell line, potential cell-specific effects are not known. However, several studies indicate that ITCs prevent several types of cancers, especially LNCaP human prostate cancer, HT29 human colon cancer, and MCF-7 human breast cancer cells (10, 32–34). NAC-AITC and NAC-sulforaphane induce biologically significant increases in the activities of Phase II xenobiotic–metabolizing enzymes, with some of them selectively modifying the proliferation of precancerous cells (6, 12). ITCs and their metabolites, such as NAC-PEITC and NAC-sulforaphane, modulate the growth of LNCaP prostate cancer cell growth and apoptosis (9, 10).

Metastasis is one of the most important factors related to cancer therapeutic efficacy and prognostic survival. One of the most active fields in cancer research is the development of novel antimetastatic drugs with low toxicity and high efficacy. In this study, we have determined adhesion and invasion to show that AITC and NAC-AITC effectively inhibit the migration of SK-Hep1 human hepatoma cells. The migration of cancer cells through a coated membrane involves not only ECM degradation but also requires the

ability of adhesive interactions between cells and the matrix. In our study, decreased migration was correlated with decreased adhesion and invasion.

Elevated expression of MMP-2/-9 is associated with increased metastatic potential in many cancers. There are no solid results regarding the extent of MMP downregulation that is effective for anticancer effects in the published literature, to our knowledge. However, we know that decreased MMP-2/-9 expression contributes to inhibition of lung metastasis of B16/F10 melanoma cells (35). Most published papers determined the downregulation of MMP by possible antimetastatic agents, not be directly measuring MMP activities. In this study, we observed up to 50%–80% downregulation of MMP-2/-9 activities by AITC and NAC-AITC compared with controls. Although this is not a direct inhibition of their enzymatic activity, this inhibition seems enough to decrease cancer metastasis, based on other studies (36, 37).

There is *in vitro* evidence that MMPs and TIMPs are critical in determining the invasive potential of proliferating tumor cells. MMP-2 and -9 are necessary for the migration of many normal cell types and tumor cells (38). Broccoli and watercress extracts (0.1–1 mg/ml) suppressed 12-O-tetradecanoylphorbol-13-acetate–induced MMP-9 activity and invasion in human MDA-MB-231 breast cancer cells (39). Benzyl ITC, one of the ITCs, also inhibited MMP-9 secretion in vascular smooth-muscle cells (40). These results support that hypothesis that dietary intake of cruciferous vegetables is associated with antimetastatic potential. The migration of cancer cells is inhibited by TIMP-1 and -2. It has been reported that TIMP-1 may play an important role in growth and migration, especially of hepatocellular carcinomas (41). We have demonstrated that AITC and NAC-AITC suppressed the MMP-2/-9 activities in terms of both protein and mRNA levels and eventually inhibited cancer cell metastasis. This conclusion is in agreement with those of previous studies, that inhibitors of MMP-2 significantly suppress tumor metastasis in experimental animals (42). However, our results show that control, AITC-treated, and NAC-AITC–treated SK-Hep1 cells expressed *TIMP*-1/-2 mRNA, and that there were no dose-response relationships among these treatments.

Several studies have found that, depending on the tumor, both increased and decreased TIMP concentrations are possible. For example, increased *TIMP*-1 mRNA levels were correlated with metastasis in colorectal cancer, whereas decreased levels were found in pancreatic cancer (43). Decreased TIMP-1 and -2 levels were reported in prostate cancer, depending on the tumor grade (as quantified as the Gleason sum; Refs. 44). Other cell culture studies of cocultures of prostate cancer cells with stromal cells showed that the increased expression of pro-MMP-9 in prostate cancer cells and the downregulated expression of TIMPs in stromal cells result from differential regulation of these components, mediated by a soluble factor in the conditioned medium (45).

Considering the epidemiologic evidence that the consumption of cruciferous vegetables is associated with a reduced incidence of cancer, AITC and NAC-AITC may represent two of the dietary factors that are responsible for the inhibition of metastasis.

1. Lampe JW, Peterson S. Brassica, biotransformation and cancer risk: genetic polymorphisms alter the preventive effects of cruciferous vegetables. J Nutr 132:2991–2994, 2002.
2. Fenwick GR, Heaney RK. Glucosinolates and their breakdown products in cruciferous crops, foods and feeding stuffs. Food Chem 11:249–271, 1983.
3. Mennicke WH, Kral T, Krumbiegel G. Metabolism of some naturally occurring isothiocyanates in the rat. Xenobiotica 13:203–207, 1983.
4. Hwang E, Jeffery EH. Evaluation of urinary *N*-acetyl cysteinyl allyl isothiocyanate as a biomarker for intake and bioactivity of Brussels sprouts. Food Chem Toxicol 41:1817–1825, 2003.
5. Munday R, Munday CM. Selective induction of phase II enzymes in the urinary bladder of rats by allyl isothiocyanate, a compound derived from Brassica vegetables. Nutr Cancer 44:52–59, 2002.
6. Hwang E, Lee HJ. Induction of quinine reductase by allylisothiocyanate (AITC) and the *N*-acetylcysteine conjugate of AITC in Hepa1c1c7 mouse hepatoma cells. BioFactors (in press), 2006.
7. Manesh C, Kuttan G. Effect of naturally occurring allyl and phenyl isothiocyanates in the inhibition of experimental pulmonary metastasis induced by B16F-10 melanoma cells. Fitoterapia 74:355–363, 2003.
8. Conaway CC, Yang YM, Chung F-L. Isothiocyanates as cancer chemopreventive agents: their biological activities and metabolism in rodents and humans. Curr Drug Metab 3:233–255, 2002.
9. Chiao JW, Chung F-L, Kancherla R, Ahmed T, Mittelman A, Conaway CC. Sulforaphane and its metabolite mediate growth arrest and apoptosis in human prostate cancer cells. Int J Oncol 20:631–636, 2002.
10. Chiao JW, Chung F-L, Krzeminski J, Amin S, Ashad R, Ahmed T, Conaway CC. Modulation of growth of prostate cancer cells by the *N*-acetylcysteine conjugate of phenethyl isothiocyanate. Int J Oncol 16: 1215–1219, 2000.
11. Chiao JW, Wu H, Ramaswamy G, Conaway CC, Chung F-L, Wang L, Liu D. Ingestion of an isothiocyanate metabolite from cruciferous vegetables inhibits growth of human prostate cancer cell xenografts by apoptosis and cell cycle arrest. Carcinogenesis 25:1403–1408, 2004.
12. Hwang E, Jeffery EH. Induction of quinine reductase by sulforaphane and sulforaphane *N*-acetylcysteine conjugate in murine hepatoma cells. J Med Food 8:198–203, 2005.
13. Hecht SS, Upadhyaya P, Wang M, Bliss RL, McIntee EJ, Kenney PM. Inhibition of lung tumorigenesis in A/J mice by *N*-acetyl-S-(*N*-2-phenethylthiocarbamoyl)-L-cysteine and *myo*-inositol, individually and in combination. Carcinogenesis 23:1455–1461, 2002.
14. Price JT, Thompson EW. Mechanisms of tumour invasion and metastasis: emerging targets for therapy. Expert Opin Ther Targets 6: 217–233, 2002.
15. Simpson-Haidaris PJ, Rybarczyk B. Tumors and fibrinogen. The role of fibrinogen as an extracellular matrix protein. Ann N Y Acad Sci 936: 406–425, 2001.16. Klein G, Vellenga E, Fraaije MW, Kamps WA, de Bont ES. The possible role of matrix metalloproteinase (MMP)-2 and MMP-9 in cancer, e.g. acute leukemia. Crit Rev Oncol Hematol 50:87–100, 2004.
16. Zucker S, Vacirca J. Role of matrix metalloproteinases (MMPs) in colorectal cancer. Cancer Metastasis Rev 23:101–117, 2004.
17. Vincent MP. The matrix metalloproteinase (MMP) and tissue inhibitor of metalloproteinase (TIMP) genes. Transcriptional and posttranscriptional regulation, signal transduction and cell-type-specific expression. Methods Mol Biol 151:121–148, 2001.

18. Combourieu B, Elfol L, Delort A-M, Rabot S. Identification of new derivatives of sinigrin and glucotropaeolin produced by the human digestive microflora using ^{1}H NMR spectroscopy analysis of in vitro incubations. Drug Metab Dispos 29:1440–1445, 2001.
19. Chambers AF, Matrisian LM. Changing views of the role of matrix metalloproteinases in metastasis. J Natl Cancer Inst 89:1260–1383, 1997.
20. Hojilla CV, Mohammed FF, Khokha R. Matrix metalloproteinases and their tissue inhibitors direct cell fate during cancer development. Br J Cancer 17:1817–1821, 2003.
21. Gomez DE, Alonso DF, Yoshiji H, Thorgeirsson UP. Tissue inhibitors of metalloproteinases: structure, regulation and biological functions. Eur J Cell Biol 74:111–122, 1997.
22. Powell WC, Knox JD, Navre M, Grogan TM, Kittelson J, Nagle RB, Bowden GT. Expression of the metalloproteinase matrilysin in DU-145 cells increases their invasive potential in severe combined immunodeficient mice. Cancer Res 53:417–422, 1993.
23. Lokeshwar BL, Selzer MG, Zhu BQ, Block NL, Golub LM. Inhibition of cell proliferation, invasion, tumor growth and metastasis by an oral non-antimicrobial tetracycline analog (COL-3) in a metastatic prostate cancer model. Int J Cancer 98:297–309, 2002.
24. Cao J, Chiarelli C, Kozarekar P, Adler HL. Membrane type 1-matrix metalloproteinase promotes human prostate cancer invasion and metastasis. Thromb Haemost 93:770–778, 2005.
25. Sehgall I, Forbes K, Webb MA. Reduced secretion of MMPs, plasminogen activators and TIMPS from prostate cancer cells derived by repeated metastasis. Anticancer Res 23:39–42, 2003.
26. Lichtinghagen R, Musholt PB, Lein M, Romer A, Rudolph B, Kristiansen G, Hauptmann S, Schnorr D, Loening SA, Jung K. Different mRNA and protein expression of matrix metalloproteinases 2 and 9 and tissue inhibitor of metalloproteinases 1 in benign and malignant prostate tissue. Eur Urol 42:398–406, 2002.
27. Riddick AC, Shukla CJ, Pennington CJ, Bass R, Nuttall RK, Hogan A, Sethia KK, Ellis V, Collins AT, Maitland NJ, Ball RY, Edwards DR. Identification of degradome components associated with prostate cancer progression by expression analysis of human prostatic tissues. Br J Cancer 92:2171–2180, 2005.
28. Wilson MJ, Sellers RG, Wiehr C, Melamud O, Pei D, Peehl DM. Expression of matrix metalloproteinase-2 and -9 and their inhibitors, tissue inhibitor of metalloproteinase-1 and -2, in primary cultures of human prostatic stromal and epithelial cells. J Cell Physiol 191:208–216, 2002.
29. Liu XH, Rose DP. Suppression of type IV collagenase in MDA-MB-435 human breast cancer cells by eicosapentaenoic acid in vitro and in vivo. Cancer Lett 92:21–26, 1995.
30. Rouzaud G, Young SA, Duncan AJ. Hydrolysis of glucosinolates to isothiocyanates after ingestion of raw or microwaved cabbage by human volunteers. Cancer Epidemiol Biomarkers Prev 13:125–131, 2004.
31. Tseng E, Scott-Ramsay EA, Morris ME. Dietary organic isothiocyanates are cytotoxic in human breast cancer MCF-7 and mammary epithelial MCF-12A cell lines. Exp Biol Med 229:835–842, 2004.
32. Parnaud G, Li P, Cassar G, Rouimi P, Tulliez J, Combaret L, Gamet-Payrastre L. Mechanism of sulforaphane-induced cell cycle arrest and apoptosis in human colon cancer cells. Nutr Cancer 48:198–206, 2004.
33. Xiao D, Choi S, Lee YJ, Singh SV. Role of mitogen-activated protein kinases in phenethyl isothiocyanate-induced apoptosis in human prostate cancer cells. Mol Carcinog 43:130–140, 2005.
34. Huang SC, Ho CT, Lin-Shiau SY, Lin JK. Carnosol inhibits the invasion of B16/F10 mouse melanoma cells by suppressing metalloproteinase-9 through down-regulating nuclear factor-kappa B and c-Jun. Biochem Pharmacol 69:221–232, 2005.
35. Rudek MA, Venitz J, Figg WD. Matrix metalloproteinase inhibitors: do they have a place in anticancer therapy? Pharmacotherapy 22:705–720, 2002.
36. Mannello F, Tonti G, Papa S. Matrix metalloproteinase inhibitors as anticancer therapeutics. Curr Cancer Drug Targets 5:285–298, 2005.
37. Ratzinger G, Stoitzner P, Ebner S, Lutz MB, Layton GT, Rainer C, Senior RM, Shipley JM, Fritsch P, Schuler G, Romani N. Matrix metalloproteinases 9 and 2 are necessary for the migration of Langerhans cells and dermal dentritic cells from human and murine skin. J Immunol 168:4361–4371, 2002.
38. Rose P, Huang Q, Ong CN, Whiteman M. Broccoli and watercress suppress matrix metalloproteinase-9 activity and invasiveness of human MDA-MA-231 breast cancer cells. Toxicol Appli Pharm 209:105–113, 2005.
39. Lee J-Y, Moon S-K, Hwang C-W, Nam K-S, Kim Y-K, Yoon H-D, Kim M-G, Kim C-H. A novel function of benzyl isothiocyanate in vascular smooth muscle cells: the role of ERK1/2, cell cycle regulation, and matrix metalloproteinase-9. J. Cell Physiol 203:493–500, 2005.
40. Nakatsukasa H, Ashida K, Higashi T, Ohguchi S, Tsuboi S, Hino N, Nouso K, Urabe Y, Kinugasa N, Yoshida K, Uematsu S, Ishizaki M, Kobayashi Y, Tsuji T. Cellular distribution of transcripts for tissue inhibitor of metalloproteinases 1 and 2 in human hepatocellular carcinomas. Hepatology 24:82–88, 1996.
41. Kruger A, Arlt MJ, Gerg M, Kopitz C, Bernard MM, Chang M, Mobashery S, Fridman R. Antimetastatic activity of a novel mechanism-based gelatinase inhibitor. Cancer Res 65:3523–3526, 2005.
42. Bramhall SR, Stamp GW, Dunn J, Lemoine NR, Neoptolemos JP. Expression of collagenase (MMP-2), stromelysin (MMP-3) and tissue inhibitor of the metalloproteinases (TIMP-1) in pancreatic and ampullary disease. Br J Cancer 73:972–978, 1996.
43. Wood M, Fudge K, Mohler JL, Frost AR, Garcia F, Wang M, Stearns ME. In situ hybridization studies of metalloproteinase 2 and 9 and TIMP-1 and TIMP-2 expression in human prostate cancer. Clin Exp Metastasis 15:246–258, 1997.
44. Dong Z, Nemeth ZA, Cher ML, Palmer KC, Bright RC, Fridman R. Differential regulation of matrix metalloproteinase-9, tissue inhibitor of metalloproteinase-1 (TIMP-1) and TIMP-2 expression in co-cultures of prostate cancer and stromal cells. Int J Cancer 93:507–515, 2001.